Journal of Sound and Vibration 325 (2009) 923–937

Contents lists available at ScienceDirect

Journal of Sound and Vibration

journal homepage: www.elsevier.com/locate/jsvi

Explanation on the importance of narrow-band random excitation characters in the response of a cantilever beam

Z.H. Feng *, X.J. Lan, X.D. Zhu

Department of Mechanical Engineering, Soochow University, Suzhou 215021, People's Republic of China

ARTICLE INFO

Article history:
Received 10 September 2008
Received in revised form
22 January 2009
Accepted 4 April 2009
Handling Editor: L.G. Tham
Available online 14 May 2009

ABSTRACT

A detailed theoretical investigation into the first- and second-mode response of a parametrically excited slender cantilever beam, where, the narrow-band random excitation characters are taken into consideration, is presented. The method of multiple scales is used to determine a uniform first-order expansion of the solution of the nonlinear integro-differential equations. The first-order moment frequency- and force–response data (curves) of a specimen beam tested by other investigators are obtained. Further comparisons have been made and results show that whether the first-order moment frequency–response data (curves) or the first-order moment force–response data (curves) of the first two modes are all in agreement with other investigators' experimental results. Furthermore, the stochastic jump and bifurcation have been investigated for the first modal parametric principal resonance by using the stationary joint probability of amplitude and phase. Results show that stochastic jump occurs mainly in the region of triple-valued solution. For the frequency–response domain, if the bandwidth γ is a variable and others keep constant, the basic phenomena indicate that the most probable motion is around the higher branch when the bandwidth is smaller, whereas the most probable motion gradually approaches the lower one when the bandwidth becomes higher; if the excitation central frequency f is a variable and others keep constant, the basic phenomena imply that the higher is f, the more probable is the jump from the higher branch to the lower one once f exceeds an certain value. For the force–response domain, there is a region of excitation acceleration a within which the joint probability density has two peaks: an upper peak and a lower peak. Results show that the upper peak decreases while the lower peak increases as the value of a decreases.

1. Introduction

Slender beams subject to base excitation can find application in the modeling of many engineering fields such as tall buildings, robotic manipulators, components of high-speed machinery, pole masts, accelerating missiles, appendages of aircrafts, spacecrafts or even vehicles, etc. Hence, great attention has been paid to the nonlinear dynamics of beams subject to axially base excitation in a number of technical papers over the past few decades due to both theoretic and practical demands.

* Corresponding author. Tel.: +86 512 67269959; fax: +86 512 67165607.
E-mail address: zhfeng@suda.edu.cn (Z.H. Feng).

0022-460X/$ - see front matter © 2009 Elsevier Ltd. All rights reserved.
doi:10.1016/j.jsv.2009.04.014

By taking the nonlinear inertia terms into account and considering linear curvature in the differential equations of motion, Haight and King [1] obtained the planar frequency–response curves of a parametrically excited rod by means of averaging method. Evensen and Even-Iwanowski [2] and Nayfeh and Mook [3] investigated the nonlinear dynamics of beams only by taking the nonlinear inertia and stretching terms into consideration. Crespo da Silva and Glynn [4,5] derived a set of integro-partial-differential equations governing flexural–flexural–torsional motions of inextensional beams, including geometric and inertia nonlinearities. Their results showed that the generally neglected nonlinear terms due to curvature are of the same order as the nonlinear terms due to inertia and that the curvature terms may have a significant influence on the response of the system. Moreover, they used these equations to study nonplanar oscillations of a cantilever beam with asymmetric support conditions [6]. Crespo da Silva [7] developed equations governing flexural–flexural–torsional beams, including geometric and inertia nonlinearities and used these equation to investigate the nonlinear response of an extensional beam to a primary resonant excitation [8]. Nayfeh and Pai [9] and Pai and Nayfeh [10] used the equation of motion formulated in Ref. [4] to analyze the nonlinear vibration of a cantilever beam subject to principal parametric and primary excitations and found that the geometric nonlinear terms have a hardening effect, whereas the inertia terms have a softening effect. Their results also indicated that for the first mode the effective nonlinearity is of the hardening type, whereas for the second and higher modes the effective nonlinearity is of the softening type [9]. Arafat et al. [11] showed that the equations of motion in Ref. [4] can be derived by using Hamilton's extended principle from a Lagrangian and virtual work term. In order to verify some theoretical results aforementioned, Anderson et al. [12] experimentally investigated the only planar response of a parametrically excited slender inextensional cantilever beam based on the analytical model in Ref. [4]. Their study showed that the experimental and theoretical results are in agreement on both the frequency–response and force–response curves of the first two modes when the damping was composed of linear viscous and quadratic terms. Zavodney and Nayfeh [13] derived the nonlinear partial differential equation for a slender cantilever beam carrying a lumped mass at an arbitrary position. They compared the resulting planner version of the equations with those in Ref. [4] and found no difference between these two modeling methods. Following the equation of motion of the beam described in Ref. [13], Kar and Dwivedy [14] and Dwivedy and Kar [15–19] systematically dealt with the nonlinear dynamic behaviors of a slender beam carrying a lumped mass with principal parametric, combination parametric and internal resonance of the lower modes. Furthermore, Kane et al. [20] presented a comprehensive theory for dealing with small vibration of a general beam attached to a base undergoing an arbitrary, prescribed motion based on Kane's method. Subsequently, Yoo et al. [21] introduced a stretch deformation variable and developed the modeling results in Ref. [20]. Hyun and Yoo [22] systematically investigated the dynamic stability of the trivial response of an axially oscillating cantilever beam based on the modeling method in Refs. [20,21]. Especially, Oueini and Nayfeh [23] considered the problem of suppressing the vibration of a cantilever beam when subjected to a principal parametric resonance using a nonlinear control law with cubic velocity feedback. Their analysis revealed that cubic velocity feedback reduces the amplitude of the response and it leads to the elimination of the saddle-node bifurcation in the frequency- and force-response curves. Also, their theoretical analysis was verified experimentally. Alhazza et al. [24] presented a comprehensive investigation of the effect of time delays on the nonlinear control of parametrically excited cantilever beams. Their results showed that, when manifested in the feedback, even the minute amount of delays can completely alter the behavior and stability of the beam, leading to unexpected behavior and response. Although investigations on the nonlinear dynamics of beams subject to base excitation have received considerable attention, the (parametric) excitation to beams aforementioned was mainly restricted to be deterministic and the significance of random (parametric) excitation, especially narrow-band random (parametric) excitation, has not been highlighted. At least, from point of engineering view, a pure deterministic excitation is hard to implement.

References to narrow-band random excitation oscillators are few up to now and many related research objects are mainly concentrated on some classical oscillators such as Duffing oscillator, van der Pol oscillator, Duffing–van der Pol oscillator [25–33]. Zhu [34] thought that the study of the random parametrically excited systems were more important than that of random externally excited ones and were more difficult in theory. Huang and Zhu [35] used the stochastic averaging method and focused on quasi-integrable Hamiltonian systems under combined harmonic and white noise excitations. They solved the averaged FPK equation by using the finite difference method and also examined the stochastic jump and its bifurcation as the system parameters change. Similarly, Huang and Zhu [36] used the same method to investigate the same systems as those in Ref. [35] under bounded noise excitations. They solved the FPK equation by using the finite difference method and found that the analytical results were in good agreement with those from digital simulation of original system. Choosing the slender beams as research objects, Feng and Hu [37] studied the almost sure stability of the trivial response of flexible beams undergoing a large linear motion, in which the system was subject to narrow-band random parametric excitation with 3:1 internal resonance. Recently, Feng et al. [38] focused on the case where a slender cantilever beam was subject to axial narrow-band random excitation and investigated the largest Lyapunov exponent which determines the almost sure stability of the trivial solution, the first- and second-order non-trivial steady state response when the bandwidth was very small, and the stochastic jump and bifurcation of the first and second modal parametric principal resonance, of the system for the first time.

In this paper, we base our model on the nonlinear integro-differential equations described in Ref. [4] and extend the work of Ref. [38]. The method of multiple scales is used to determine a uniform first-order expansion of the solution of equations. We numerically obtain the first-order moment frequency–response and force–response data (curves) of the same specimen as that tested in Ref. [12] when the excitation is a narrow-band random one. Further comparisons between

present numerical data and the experimental results investigated in Ref. [12] have been made. Furthermore, the stochastic jump and bifurcation have been investigated for the first mode parametric principal resonance by using the stationary joint probability of amplitude and phase to characterize the number, location, shape and magnitude of the peaks of the stationary joint probability density.

2. Problem descriptions and analysis

Following Crespo da Silva and Glynn [4], we base our model on the nonlinear integro-differential equations to describe and investigate the only planar motion of an isotropic inextensible Euler-Bernoulli cantilever beam which is vertically mounted on a base (for instance, a modal shaker) and shown in Fig. 1, that is

$$\rho A\ddot{w} + c\dot{w} + EIw^{iv} = -EI[w'(w'w'')']'$$

$$-\frac{1}{2}\rho A\left[w'\int_L^s\left(\frac{\partial^2}{\partial t^2}\int_0^s w'^2\,\mathrm{d}s\right)\mathrm{d}s\right]' - \rho A[w''(s-L)+w'](\ddot{z}-g), \tag{1}$$

$$w = w' = 0 \quad \text{at } s = 0 \tag{2a}$$

$$w'' = w''' = 0 \quad \text{at } s = L, \tag{2b}$$

where w is the transverse displacement; the primes and overdots indicate the derivative with respect to the arc length s and time t, respectively; ρ is the beam density; A is the cross-sectional area; c is the coefficient of linear viscous damping per unit length; E is Young's modulus of elasticity; I is the moment of inertia about the neutral axis of the beam; L is the constrained length of the beam; $\ddot{z}$ is the parametric excitation acceleration of the base; and g is the gravity acceleration.

Here the beam has been assumed to be weakly nonlinear and retained only up to cubic nonlinearlities.

In most studies of the nonlinear dynamics of aforementioned beams, the base motion is almost the same case, i.e., a pure harmonic excitation. From the point of theoretical view, such a harmonic excitation assumption is unquestionable so that it is widely considered and introduced by most investigators. From the point of technical or engineering view, however, we need to elaborate on the excitation because it is hard for a structure to experience a pure and long-term harmonic excitation, on other words, such a harmonic excitation assumption needs to be modified more or less. For instance, Anderson et al. [12] experimentally investigated the planar response of a parametrically excited cantilever beam. They used a signal generator and a power amplifier to drive a 250 lb modal shaker with a custom table and suspension to allow base excitation. In order to capture the experimental frequency–response and force–response curves for the first and second modal principal parametric resonance (within a very narrow frequency extent), the base motion was along the axis of the beam at constant acceleration amplitude and a fixed frequency (forward sweep or reverse sweep). Results in Figs. 3, 7, 9 and 13 in their research show that the frequency–response curve is a definite overhang, in other words, jumps from the higher branch (nontrivial) to the lower one (trivial) or from the lower branch to the higher one occur. In order to explain these phenomena in theory, they assumed that the damping is composed of linear viscous and quadratic terms. Their research show that adding quadratic damping in the analysis improves qualitatively as well as quantitatively the agreement between the experimental and theoretical results, which, indeed indicates the rationality from one side to some extent. On the other hand, however, there exist two discussible problems. At first, adding quadratic damping is only suitable for the situation where the relative velocity between the moving body and the liquid with weak viscidity is not lower; in fact, the first two natural frequencies of the beam (test specimen) in Ref. [12] are only about 0.66 and 5.69 Hz, respectively. Secondly, in the point of technical view, it is very difficult to keep the excitation frequency of the shaker at a fixed one to experience a long-term excitation. In other words, the excitation frequency will slightly drift off the center

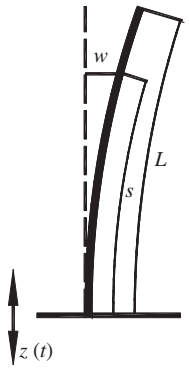

Fig. 1. Configuration of a cantilever beam subject to a vertical base excitation.

(fixed) frequency in random and such a harmonic excitation in fact is not a pure harmonic one and may be treated as a narrow-band stochastic process. Thus, the definite overhang or jumping phenomena in their experimental results can be explained and described using the theory of random vibration and their experimentally investigated jump may be the stochastic jump in nature.

Currently, there are two kinds of models for the description of narrow-band random excitation. One is the response of second-order linear filter to Gaussian white noise. The other is the so-called bounded noise. The latter is a harmonic function with constant amplitude and stochastic frequency and phase, which, to some extent, can be used to describe the excitation situation where a modal shaker is driven at constant acceleration amplitude and a center frequency with slight flutter. The bounded noise process was first proposed by Stratonovich [39] and has been used and developed by some researchers in certain applications [40–47].

Following Ref. [38], in what follows, we use the bounded narrow-band noise to feature the aforementioned narrow-band random excitation, that is

$$\ddot{z}(t) = \xi(t) = a\cos(\Omega t + \gamma W(t) + \theta), \tag{3}$$

where a and Ω are the acceleration amplitude and center circular frequency of the base motion , which are constants, $\gamma \geqslant 0$ is a intensity, which represents the bandwidth, of the narrow-band random excitation, $W(t)$ is a standard Wiener process, and θ is a uniformly distributed random number in $[0,2\pi]$. The inclusion of the phase angle θ makes $\xi(t)$ a stationary process. So $\xi(t)$ is a non-Gaussian distributed stationary stochastic process and has density function $p(\xi) = 1/(\pi\sqrt{a^2-\xi^2})$, zero mean value and spectral density function as follows:

$$S_\xi(\omega) = \frac{1}{4\pi}\frac{a^2\gamma^2(\Omega^2+\omega^2+\gamma^2/4)}{(\Omega^2-\omega^2+\gamma^4/4)^2+\omega^2\gamma^4}. \tag{4}$$

Choosing proper value for a and γ, $\xi(t)$ may represent the turbulent flow in the wind, the motion of seismic floor and so on.

The bandwidth of process $\xi(t)$ depends mainly on parameter γ. It is a narrow-band process when γ is small and a wide-band process when γ is large.

In order to make further comparison with Ref. [12], we nondimensionlize Eqs. (1)–(2) using the characteristic length $l_n = L/\lambda_n$ of the beam and the characteristic time $\tau_n = (L/\lambda_n)^2\sqrt{\rho A/EI}$ as the same as those in Ref. [12], where λ_n is the nth root of the characteristic equation $1+\cos(\lambda_n)\cosh(\lambda_n) = 0$. Let the nondimensional arc length $x = s/l_n$ and the nondimensional time $\tau = t/\tau_n$, we have

$$\ddot{v} + \varepsilon^2\mu\dot{v} + v^{iv} = -(v'(v'v'')')' - \frac{1}{2}\left[v'\int_{\lambda_n}^{x}\frac{\partial^2}{\partial\tau^2}\left(\int_0^x v'^2\,\mathrm{d}x\right)\mathrm{d}x\right]' - \varepsilon^2[v''(x-\lambda_n) + v'](\ddot{z}_b - g_b), \tag{5}$$

where the primes and overdots indicate the derivative with respect to x and τ, respectively; $v = w/l_n$, $\varepsilon^2\mu = c\tau_n/(\rho A)$, $\varepsilon^2\ddot{z}_b = \ddot{z}\tau_n^2/l_n$ and $\varepsilon^2 g_b = g\tau_n^2/l_n$ are the corresponding nondimensional values of w, c, $\ddot{z}$ and g, respectively; and ε is a small positive parameter introduced as a bookkeeping device. The associated boundary conditions are

$$v = v' = 0 \quad \text{at } x = 0, \tag{6a}$$

$$v'' = v''' = 0 \quad \text{at } x = \lambda_n. \tag{6b}$$

Naturally, the narrow-band random excitation in Eq. (5) can also be rewritten as

$$\ddot{z}_b(\tau) = a_b\cos(\Omega_b\tau + \gamma W(\tau) + \theta), \tag{7}$$

where $a_b = a\tau_n^2/(\varepsilon^2 l_n)$ and $\Omega_b = \Omega\tau_n$ are the nondimensional acceleration amplitude and center circular frequency of the base motion.

In order to analyze the solutions of the nonlinear Eq. (5) subject to the boundary conditions (6), the method of multiple scales is employed here [25,26,31,32,37,38,48]. Thus, a first-order uniform expansion of the form is used as given below

$$v(x,T_0,T_2;\varepsilon) = \varepsilon v_1(x,T_0,T_2,\ldots) + \varepsilon^3 v_3(x,T_0,T_2,\ldots) + \ldots, \tag{8}$$

where $T_0 = \tau$ is a fast scale characterizing motions with the natural frequencies ω_n and Ω_b; and $T_2 = \varepsilon^2\tau$ is a slow scale characterizing the modulations of the amplitudes and phases. Moreover, for a standard Wiener process $W(\tau)$, because of $E[W(\tau)] = 0$ and $E[W^2(\tau)] = \tau$, we have

$$\gamma W(\tau) = (\gamma/\varepsilon)W(\varepsilon^2\tau) = \bar{\gamma}W(T_2). \tag{9}$$

Substituting Eqs. (7)–(9) into Eqs. (5) and (6) and equating coefficients of like powers of ε, we obtain

Order ε:

$$D_0^2 v_1 + v_1^{iv} = 0, \tag{10a}$$

$$v_1 = v_1' = 0 \quad \text{at } x = 0, \tag{10b}$$

$$v_1'' = v_1''' = 0 \quad x = \lambda_n. \tag{10c}$$

Order ε^3:

$$D_0^2 v_3 + v_3^{iv} = -2D_0 D_2 v_1 - \mu D_0 v_1 - (v_1'(v_1' v_1'')')' - \frac{1}{2}\left[v_1' \int_{\lambda_n}^{x} D_0^2\left(\int_0^x v_1'^2\,\mathrm{d}x\right)\mathrm{d}x\right]'$$

$$-[v_1''(x-\lambda_n) + v_1']\{a_b\cos[\Omega_b T_0 + \bar{\gamma} W(T_2) + \theta] - g_b\}, \tag{11a}$$

$$v_3 = v_3' = 0 \quad \text{at } x = 0, \tag{11b}$$

$$v_3'' = v_3''' = 0 \quad \text{at } x = \lambda_n. \tag{11c}$$

where $D_k = \partial/\partial T_k$.

The general solution of Eq. (10) consists of one infinite sequence of modes corresponding to one infinite sequence of frequencies and can be expressed in terms of the linear free-vibration modes: that is,

$$v_1(x, T_0, T_2) = \sum_{m=1}^{\infty} \Phi_m(x) A_m(T_2) \mathrm{e}^{\mathrm{i}\omega_m T_0} + cc, \tag{12}$$

where cc stands for the complex conjugate of the preceding terms, $\omega_m = \lambda_m^2/\lambda_n^2$, and

$$\Phi_m(x) = \frac{1}{\sqrt{\lambda_n}}\left\{\cosh\left(\frac{\lambda_m}{\lambda_n}x\right) - \cos\left(\frac{\lambda_m}{\lambda_n}x\right) + \frac{\cos\lambda_m + \cosh\lambda_m}{\sin\lambda_m + \sinh\lambda_m}\left[\sin\left(\frac{\lambda_m}{\lambda_n}x\right) - \sinh\left(\frac{\lambda_m}{\lambda_n}x\right)\right]\right\}.$$

Here $\Phi_m(x)$ is chosen to satisfy $\int_0^{\lambda_n} \Phi_m^2(x)\,\mathrm{d}x = 1$.

Now, our attention is paid to the case where only the nth mode is directly excited and thus it is assumed that there are not any internal resonances between two modes. Therefore, out of the infinite modes present in v_1 and in the present of viscous damping, only the excited mode will contribute to the long-term response [9–19]. Thus, the non-decaying first-order solution can be expressed as

$$v_1(x, T_0, T_2) = \Phi_n(x)[A_n(T_2)\mathrm{e}^{\mathrm{i}T_0} + \bar{A}_n(T_2)\mathrm{e}^{-\mathrm{i}T_0}]. \tag{13}$$

Substituting Eq. (13) into Eq. (11a) yields

$$\begin{aligned} D_0^2 v_3 + v_3^{iv} = & -2i\Phi_n D_2 A_n \mathrm{e}^{\mathrm{i}T_0} - \mathrm{i}\mu\Phi_n A_n \mathrm{e}^{\mathrm{i}T_0} - [\Phi_n'(\Phi_n'\Phi_n'')']'(A_n^3\mathrm{e}^{3\mathrm{i}T_0} + 3A_n^2\bar{A}_n\mathrm{e}^{\mathrm{i}T_0}) \\ & - \frac{1}{2}\left(\Phi_n' \int_{\lambda_n}^{x}\int_0^x \Phi_n'^2\,\mathrm{d}x\,\mathrm{d}x\right)'(-4A_n^3\omega_n^2\mathrm{e}^{3\mathrm{i}T_0} - 4A_n^2\bar{A}_n\omega_n^2\mathrm{e}^{\mathrm{i}T_0}) + [\Phi_n''(x-\lambda_n) + \Phi_n']g_b A_n \mathrm{e}^{\mathrm{i}T_0} \\ & - \frac{a_b}{2}[\Phi_n''(x-\lambda_n) + \Phi_n']\{A_n\mathrm{e}^{\mathrm{i}[(\Omega_b+1)T_0+\gamma W+\theta]} + \bar{A}_n\mathrm{e}^{\mathrm{i}[(\Omega_b-1)T_0+\bar{\gamma}W+\theta]}\} + cc. \end{aligned} \tag{14}$$

Similar to Ref. [12], here we restrict our discussion and investigation to the case of principal parametric resonance of nth mode (i.e., $\Omega_b \approx 2$). Thus, the frequency detuning parameter σ is introduced to describe the closeness to the nth modal principal parametric resonance as given below

$$\Omega_b = 2 + \varepsilon^2\sigma. \tag{15}$$

According to the definition of the solvability conditions described in Ref. [38], we have

$$\begin{aligned} & \int_0^{\lambda_n}\left\{-\mathrm{i}\Phi_n(2D_2A_n + \mu A_n) - \left[3(\Phi_n'(\Phi_n'\Phi_n'')')' - 2\left(\Phi_n'\int_{\lambda_n}^{x}\int_0^x \Phi_n'^2\,\mathrm{d}x\,\mathrm{d}x\right)'\right]A_n^2\bar{A}_n\right\}\Phi_n\,\mathrm{d}x \\ & + \int_0^{\lambda_n} g_b A_n[\Phi_n''(x-\lambda_n) + \Phi_n']\Phi_n\,\mathrm{d}x - \int_0^{\lambda_n}\frac{a_b}{2}\bar{A}_n[\Phi_n''(x-\lambda_n) + \Phi_n']\mathrm{e}^{\mathrm{i}(\sigma T_2 + \bar{\gamma}W + \theta)}\Phi_n\,\mathrm{d}x = 0 \end{aligned} \tag{16}$$

which yields

$$-2\mathrm{i}D_2A_n - \mathrm{i}\mu A_n - (3\alpha_1 - 4\alpha_2)A_n^2\bar{A}_n + \alpha_3 A_n g_b - \frac{a_b}{2}\alpha_3\bar{A}_n\mathrm{e}^{\mathrm{i}(\sigma T_2 + \bar{\gamma}W + \theta)} = 0, \tag{17}$$

where $\alpha_1 = \int_0^{\lambda_n}\Phi_n(\Phi_n'(\Phi_n'\Phi_n'')')'\,\mathrm{d}x$, $\alpha_2 = 1/2\int_0^{\lambda_n}\Phi_n(\Phi_n'\int_{\lambda_n}^{x}\int_0^x\Phi_n'^2\,\mathrm{d}x\,\mathrm{d}x)'\,\mathrm{d}x$, and $\alpha_3 = \int_0^{\lambda_n}\Phi_n[\Phi_n''(x-\lambda_n) + \Phi_n']\,\mathrm{d}x$.

We can find that the forms of α_1, α_2, and α_3 in Eq. (17) are the same as those in Eq. (22) of Ref. [12] and these corresponding numerical values are given in Table 1 for the first two modes, which are almost the same as those in Table 1 of Ref. [12] except α_1 for the first mode. In fact, if α_1 is 0.462 for the first mode in Table 1 of Ref. [12], the theoretical frequency–response curves in Figs. 3, 5, and 7 of Ref. [12] will be bent to left, i.e., these curves will present softening effect. For this reason, $\alpha_1 = 0.462$ for the first mode in Table 1 of Ref. [12] must be either a typing error or a calculating error.

Substituting the polar form

$$A_n(T_2) = \tfrac{1}{2}a_n(T_2)\mathrm{e}^{\mathrm{i}[\sigma T_2 - \theta_n(T_2)]/2}, \tag{18}$$

Table 1
Values of coefficients in modulation equations.

	First mode	Second mode
α_1	0.4962	0.2672
α_2	0.3486	0.6996
α_3	0.8378	1.8421

Table 2
Nondimensional time, gravity acceleration and excitation acceleration.

	First mode	Second mode
τ_n	0.1703	0.0272
$\varepsilon^2 a_b$	0.0754	0.0064
$\varepsilon^2 g_b$	0.6255	0.0399

into Eq. (17) and separating the real and imaginary parts, we obtain

$$\dot{a}_n = -\tfrac{1}{2}\mu a_n - \tfrac{1}{4}a_b\alpha_3 a_n \sin\beta_n, \tag{19a}$$

$$a_n\dot{\beta}_n = \sigma a_n - (\tfrac{3}{4}\alpha_1 - \alpha_2)a_n^3 - \tfrac{1}{2}a_b\alpha_3 a_n \cos\beta_n + \alpha_3 g_b a_n + a_n\bar{\gamma}\dot{W}, \tag{19b}$$

where $\beta_n = \theta_n + \gamma W + \theta$.

3. Numerical simulation

In what follows, the specimen (i.e., a vertically mounted carbon steel cantilever beam of dimensions 852.42 mm × 19.05 mm × 0.81 mm (33.56 in × 0.75 in × 0.032 in)) and the acceleration excitation amplitudes of the base (i.e., $a = 1182\,\text{mm/s}^2$ ($46.53\,\text{in/s}^2$) for the first mode and $a = 1569\,\text{mm/s}^2$ ($61.78\,\text{in/s}^2$) for the second mode, respectively) experimentally investigated in Ref. [12] are taken into consideration to make further investigation and comparison. Furthermore, we assume $\varepsilon^2 = 0.1$ and $\varepsilon^2\mu = 0.002$. Thus, the nondimensional time, gravity acceleration and excitation acceleration amplitude and the first four natural frequencies with or without gravity acceleration being taken into consideration are shown in Tables 2 and 3, respectively.

When $\gamma = 0$ and $\theta = 0$, the nonlinear modulation Eq. (19) can be treated as a deterministically excited system and two possible nontrivial solutions (one branch is stable and another unstable) when $a_b > 2\mu/\alpha_3$ are given below

$$a_n = \sqrt{\frac{2\sigma + 2\alpha_3 g_b \pm \sqrt{(a_b\alpha_3)^2 - (2\mu)^2}}{\frac{3}{2}\alpha_1 - 2\alpha_2}} \tag{20}$$

In Figs. 2 and 3, we show the theoretical frequency–response and force–response curves based on Eq. (20) for the first mode, respectively, where $f = \Omega/2\pi$ is the center frequency of the base motion. For all the plotted theoretical curves, solid lines indicate stable fixed points and dot lines indicate unstable fixed points. As a familiar result, Fig. 2 features the hardening type, i.e., the theoretical frequency–response curve is bent to the right, indicating that the nonlinear curvature terms dominate the nonlinear inertia terms for the first mode. In Fig. 3, we can find that the force–response curves, for instance, curves A and B, may exhibit dual-valued solution (one is stable and another is unstable. In fact, the response is triple-valued: among them there are one stable nontrivial solution, one stable trivial solution, and one unstable nontrivial solution) when the excitation central frequencies are greater than an center frequency in the unstable region (for instance, about 1.377 Hz in Fig. 2), whereas the force–response curves, for instance, curves D and E, can only exhibit stable single-valued solution when the excitation frequencies are less than the center frequency.

Similar to Figs. 2 and 3, Figs. 4 and 5 show the theoretical frequency–response and force–response curves based on Eq. (20) for the second mode, respectively. Naturally, we can find that the theoretical frequency–response curve belongs to softening type, which, results in that the force–response curves, for instance, curves A and B, may exhibit dual-valued solution when the excitation central frequencies are less than an center frequency in the unstable region (for instance, about 11.273 Hz in Fig. 4), whereas the force–response curves, for instance, curves D and E, can only exhibit stable single-valued solution when the excitation frequencies are greater than the center frequency.

Table 3
First four natural frequencies of the cantilever beam.

	With gravity (Ref. [12]) (Hz)	Without gravity (Hz)
First mode	0.66	0.95
Second mode	5.69	5.93
Third mode	16.22	16.60
Fourth mode	32.06	32.53

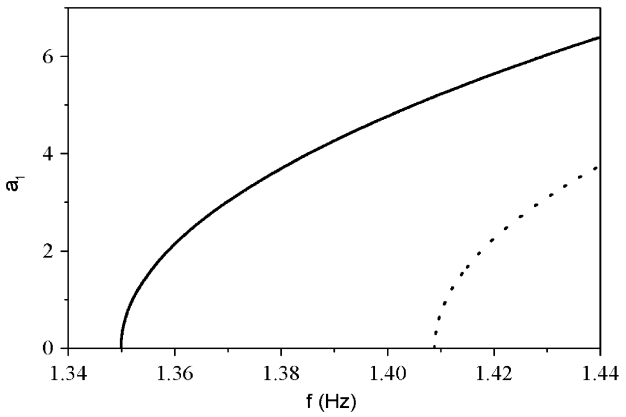

Fig. 2. Frequency–response curves for the first mode when $a = 1182\,\text{mm/s}^2$ ($46.53\,\text{in/s}^2$).

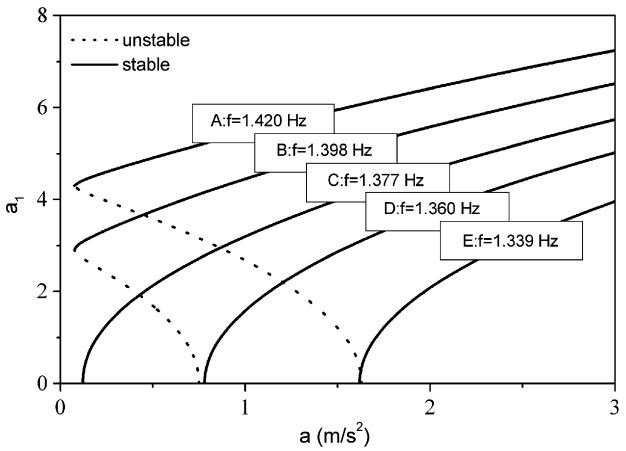

Fig. 3. Force–response curves for the first mode.

Now, we focus on the case where the excitation is a narrow-band random one. For the method of numerical calculations, Eq. (3) can be rewritten to be the form as given below

$$\ddot{z}(t) = \xi(t) = a\cos(\varphi(t)), \quad \dot{\varphi}(t) = \Omega + \gamma\varsigma(t), \quad \zeta(t) = \dot{W}(t).$$

The formal derivative $\zeta(t)$ of the unit Wiener process is a Gaussian white noise, which has the power spectrum of a constant and is physical unrealized. According to Refs. [49,50], the pseudorandom signal is used for the numerical calculations as given below

$$\zeta(t) = \sqrt{\frac{4\Omega}{N}} \sum_{k=1}^{N} \cos\left[\frac{\Omega}{N}(2k-1)t + \phi_k\right], \tag{21}$$

where ϕ_k's are independent and uniformly distributed in $(0, 2\pi]$, N is a large integer number and here we chose $N = 1000$ for the following calculation.

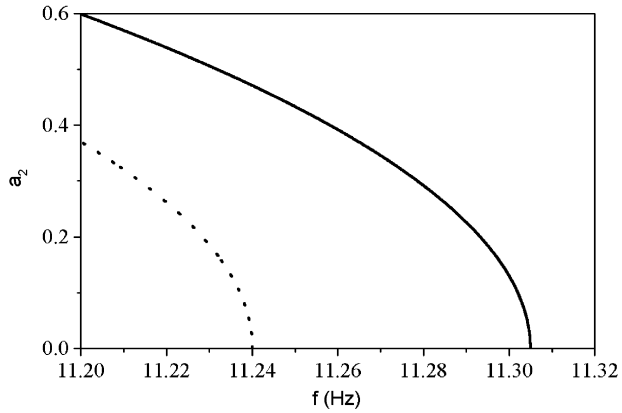

Fig. 4. Frequency–response curves for the second mode when $a = 1569\,\mathrm{mm/s^2}$ ($61.78\,\mathrm{in/s^2}$).

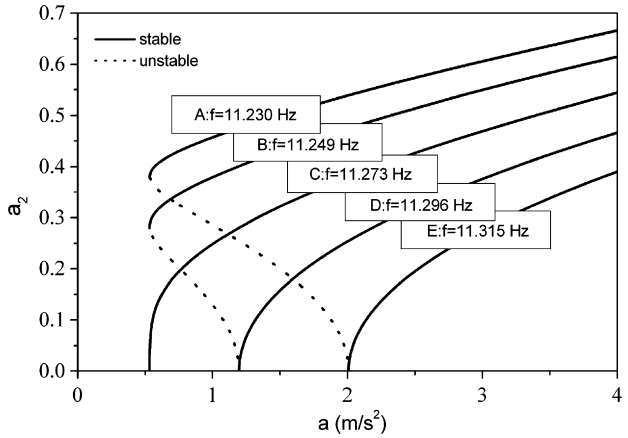

Fig. 5. Force–response curves for the second mode.

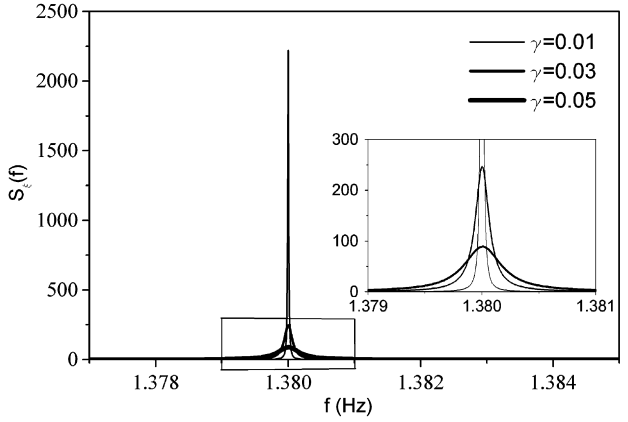

Fig. 6. Spectral density of $\xi(t)$ at $f = 1.38\,\mathrm{Hz}$ with different bandwidths.

Fig. 6 shows the spectral density of the narrow-band random excitation $\ddot{z}(t)$ when the excitation frequency f is1.38 Hz (near the center frequency of the unstable region in Fig. 2) with three different bandwidths. From this figure we can find that the bandwidth of the excitation signal is still very narrow even if $\gamma = 0.05$.

In Fig. 7, we show the theoretical frequency–response curves and the first-order moment frequency–response data (curves) numerically obtained from Eq. (19) combined with Eq. (21) for the first mode, where, the initial condition is

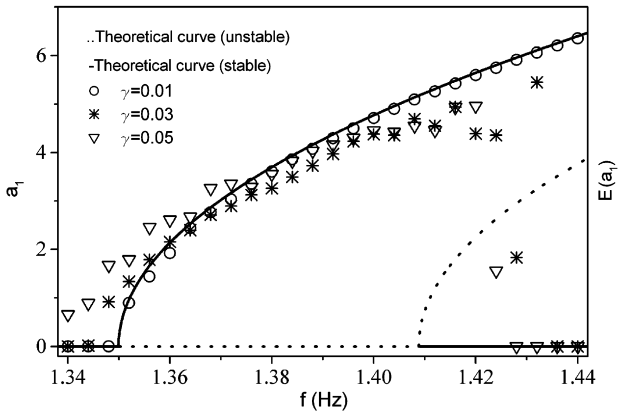

Fig. 7. Theoretical frequency–response curves and the first-order moment frequency–response data with different bandwidths for the first mode when $a = 1182\,\mathrm{mm/s^2}$ $(46.53\,\mathrm{in/s^2})$.

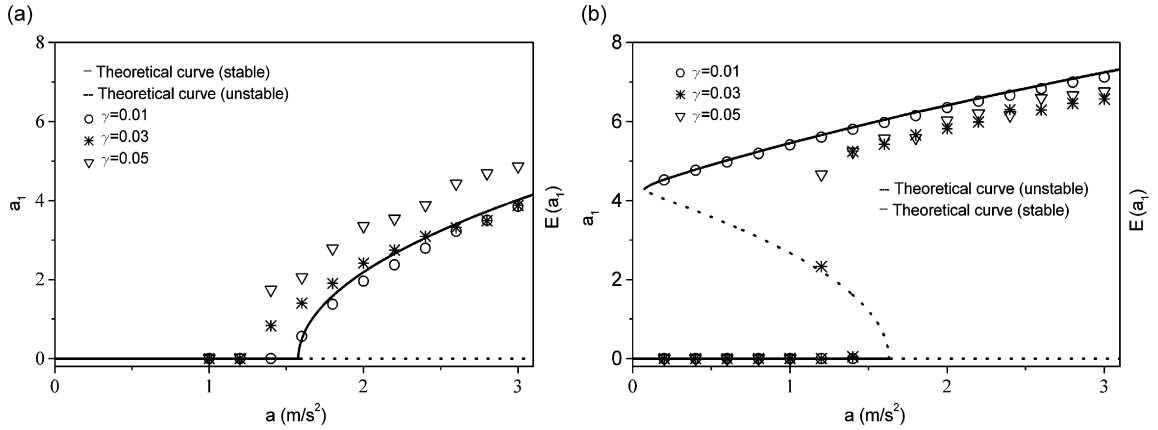

Fig. 8. Theoretical force–response curves and the first-order moment force–response data with different bandwidths for the first mode when (a) $f = 1.34\,\mathrm{Hz}$, and (b) $f = 1.42\,\mathrm{Hz}$.

$(a_1, \beta_1) = (5.0, 0)$, integrating time is 5000, and calculating time is 2500. The numerical results are also bent to the right. Also, we can find that the numerical results are at the theoretical stable curve's heels within the analytical frequency extent when the bandwidth is very narrow. However, the data (curves) gradually jump from the nontrivial branch to the trivial one when the excitation frequency exceeds the unstable region and they are obviously bounded with the increase of bandwidth. It is also more interested in that Fig. 7 is much more similar to Fig. 3 of Ref. [12]

In Fig. 8, we show the theoretical force–response curves and the first-order moment force–response data (curves) for the first mode when the excitation frequencies are 1.34 Hz (lying in the left-hand side of the unstable region of Fig. 7) and 1.42 Hz (lying in the right-hand side of the unstable region of Fig. 7), respectively. Here, the initial condition is set near either the stable nontrivial branch or the stable trivial branch, integrating time is still 5000, and calculating time is also 2500. We can amazedly find that Fig. 8(a) is also very similar to Fig. 4 of Ref. [12], where, the excitation frequency is 1.253 Hz and lies in the left-hand side of the unstable region in Fig. 3 of Ref. [12]. In Fig. 8(b), the numerical results closely encircle either the stable nontrivial branch or the stable trivial branch when the bandwidth is very narrow. With the increase of bandwidth, jumps occur between these two branches.

Fig. 9 shows the spectral density of the narrow-band random excitation $\ddot{z}(t)$ when the excitation central frequency f is11.27 Hz (near the center frequency of the unstable region in Fig. 4) with three different bandwidths. From this figure we can also find that the bandwidth of the excitation signal is much more narrow even if $\gamma = 0.03$.

In Fig. 10, we also show the theoretical frequency–response curves and the first-order moment frequency–response data (curves) numerically obtained from Eq. (19) combined with Eq. (21) for the second mode, where, the initial condition is $(a_2, \beta_2) = (0.6, 0)$, integrating time is 5000, and calculating time is 2500. The numerical results are bent to the left. Similarly, from this figure we can find the same phenomena as those in Fig. 7. It is also seen that Fig. 10 is similar to Fig. 9 of Ref. [12]. In Fig. 11, we show the theoretical force–response curves and the first-order moment force–response data (curves) for the second mode when the excitation central frequency is 11.23 Hz (lying in the left-hand side of the unstable region of Fig. 10). Here, the initial condition is also set near either the stable nontrivial branch or the stable trivial branch, integrating time is

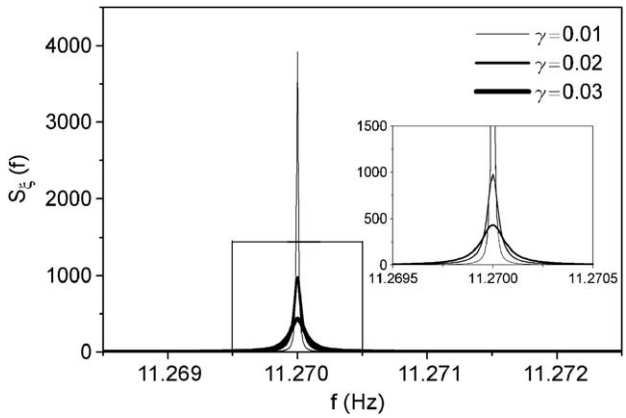

Fig. 9. Spectral density of $\xi(t)$ at $f = 11.27$ Hz with different bandwidths.

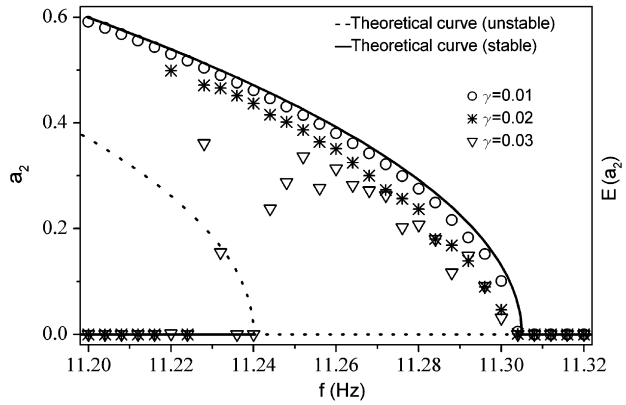

Fig. 10. Frequency–response curves and the first-order moment frequency–response data with different bandwidths for the second mode when $a = 1569\,\text{mm/s}^2$ ($61.78\,\text{in/s}^2$).

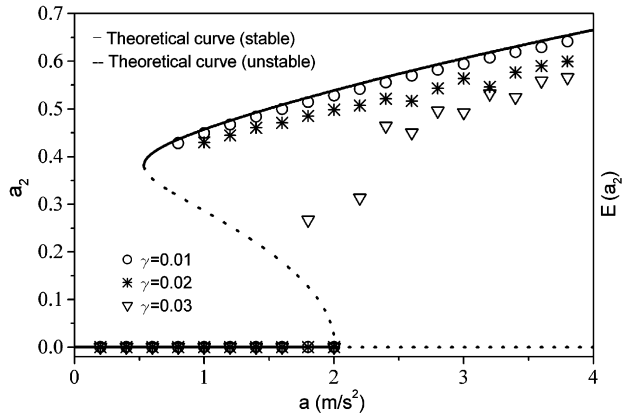

Fig. 11. Theoretical force–response curves and the first-order moment force–response data with different bandwidths for the second mode when $f = 11.23$ Hz.

still 5000, and calculating time is also 2500. Naturally, it is seen that Fig. 11 is similar to Fig. 10 of Ref. [12], where, the excitation frequency is 11.05 Hz and lies in the left-hand side of the unstable region in Fig. 9 of Ref. [12]. With the increase of bandwidth, jumps occur between the two stable branches.

The main aim we use first-order moment responses in Figs. 7, 8, 10, and 11 is to make comparison with the experimental results in Ref. [12]. In fact, there may be two more probable motions in the system. The first-order moment response aforementioned, although it is useful, is a single statistical quantity, which, is not enough to describe the complicated response, and sometimes the application of first-order moment response depends on the initial conditions, calculating time, and so on. Zhu et al. [27] thought that the jump of a system under narrow-band random excitation is essentially a transition of the response from one more probable motion to another or vice versa, and the behavior of the complicated stationary response of a nonlinear system to random excitation is best described by the stationary joint probability of variables such as displacement, velocity and so on and is characterized by the number, location, shape and magnitude of the peaks of the stationary joint probability density.

Eq. (19) is a two-dimensional diffusion process and it is more convenient to solve the FPK equation associated with its Itô equation to obtain the statistics of the response. Thus, the FPK equation associated with Eq. (19) is of the form [34]

$$\frac{\partial p}{\partial T_2} = -\frac{\partial}{\partial a_n}[m_1(a_n,\beta_n)p] - \frac{\partial}{\partial \beta_n}[m_2(a_n,\beta_n)p] + \frac{\bar{\gamma}^2}{2}\frac{\partial^2 p}{\partial \beta_n^2}, \tag{22}$$

where $p = p(a_n,\beta_n,T_2|a_{n0},\beta_{n0})$ is the transition probability density, $m_1(a_n,\beta_n) = -\frac{1}{2}\mu a_n - \frac{1}{4}a_b\alpha_3 a_n \sin\beta_n$, and $m_2(a_n,\beta_n)_n = \sigma - (\frac{3}{4}\alpha_1 - \alpha_2)a_n^2 - \frac{1}{2}a_b\alpha_3\cos\beta_n + \alpha_3 g_b$.

The initial condition of FPK Eq. (22) is

$$p = \delta(a_n - a_{n0})\delta(\beta_n - \beta_{n0}), \quad T_2 = 0.$$

The boundary condition with respect to β_n is periodic, i.e.,

$$p|_{\beta_n+2m\pi} = p|_{\beta_n}$$

$$\partial p/\partial\beta_n|_{\beta_n+2m\pi} = \partial p/\partial\beta_n|_{\beta_n}.$$

The boundary conditions with respect to a_n is

$$p = \textit{finite} \text{ at } a_n = 0,$$

$$p, \partial p/\partial a_n \to 0, \quad \text{as } a_n \to \infty.$$

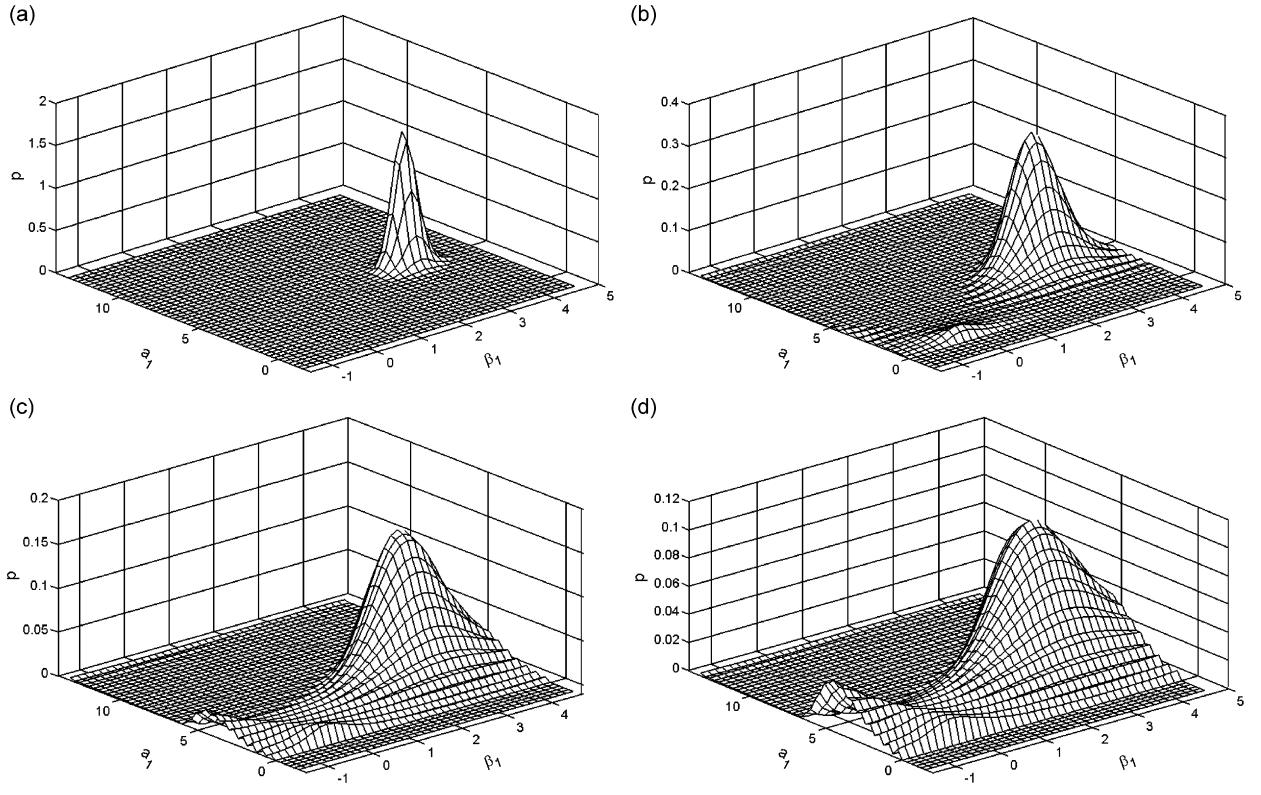

Fig. 12. Stationary joint probability density of the first mode to different bandwidth $\bar{\gamma}$: $f = 1.41$ Hz; $a = 1182$ mm/s^2 (46.53 in/s^2); (a) $\gamma = 0.005$; (b) $\gamma = 0.010$; (c) $\gamma = 0.015$; and (d) $\gamma = 0.020$.

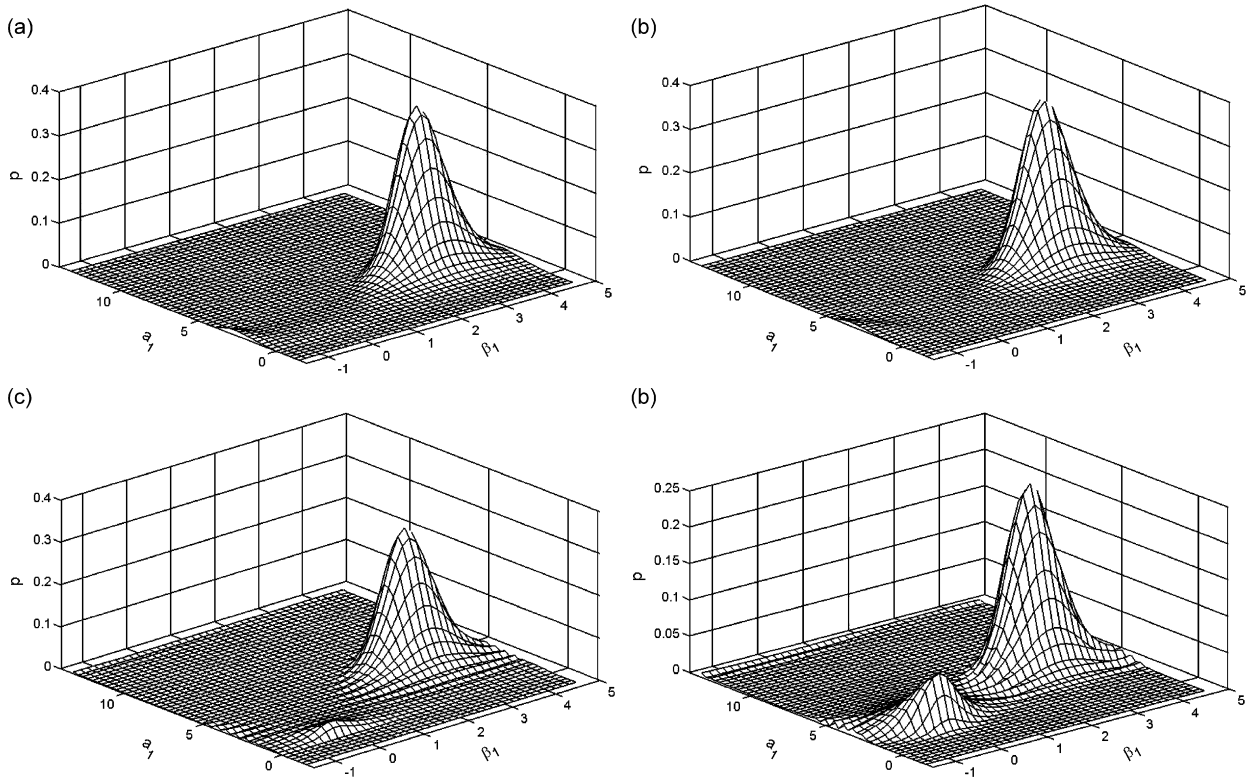

Fig. 13. Stationary joint probability density of the first mode to different frequency f: $\gamma = 0.01$; $a = 1182\,\text{mm/s}^2$ $(46.53\,\text{in/s}^2)$; (a) $f = 1.39\,\text{Hz}$; (b) $f = 1.40\,\text{Hz}$; (c) $f = 1.41\,\text{Hz}$; and (d) $f = 1.42\,\text{Hz}$.

In what follows, we mainly focus on the nonlinear dynamics of the first mode of the system to elaborate the corresponding statistical characters.

Fig. 12 shows a series of change of the stationary joint probability density of amplitude and phase for the first mode to different bandwidths numerically solved from the FPK Eq. (22) by using finite difference method when $f = 1.41\,\text{Hz}$ and $a = 1182\,\text{mm/s}^2$. Here, we choose $f = 1.41\,\text{Hz}$ so that the excitation frequency f lies in the margin of the stable region in Fig. 7. The basic jump phenomena indicate that the most probable motion is around the higher branch when the bandwidth is smaller, whereas the most probable motion gradually approaches the lower one when the bandwidth becomes higher.

Fig. 13 shows the stationary joint probability density of amplitude and phase for the first mode for four increasing values of excitation central frequency f (see Fig. 7). It is observed that there is an excitation central frequency value over which the joint probability density has two peaks: an upper peak and a lower peak. This implies that jumps may occur over the frequency value where the response is in the region of triple-valued solution. As the value of f increases, the higher peak decreases while the lower peak increases. This also implies that the higher is the excitation central frequency f, the more probable is the jump from the higher branch to the lower one once f exceeds the value.

Fig. 14 shows the stationary joint probability density of amplitude and phase for the first mode for four decreasing values of excitation acceleration a (see Fig. 8(b)). One can find that there is a region of excitation acceleration within which the joint probability density has two peaks: an upper peak and a lower peak. This implies that jumps may occur in this region of a values value where the response is also in the region of triple-valued solution. As the value of a decreases, the upper peak decreases while the lower peak increases. This indicates that the lower is the excitation acceleration a, the more probable is the jump from the higher branch to the lower one once a lies in the region.

4. Conclusions

The nonlinear integro-differential equations of motion for a slender cantilever beam subject to axial narrow-band random excitation were proposed and investigated. The method of multiple scales was used to determine a uniform first-order expansion of the solution of equations. According to solvability conditions, the nonlinear modulation equations for the principal parametric resonance were obtained.

We numerically obtained the first-order moment frequency–response and force–response data (curves) of the same specimen as that tested in Ref. [12] when the excitation is a narrow-band random one. Further comparisons between present numerical data and the experimental results investigated in Ref. [12] have been made. Results show that whether

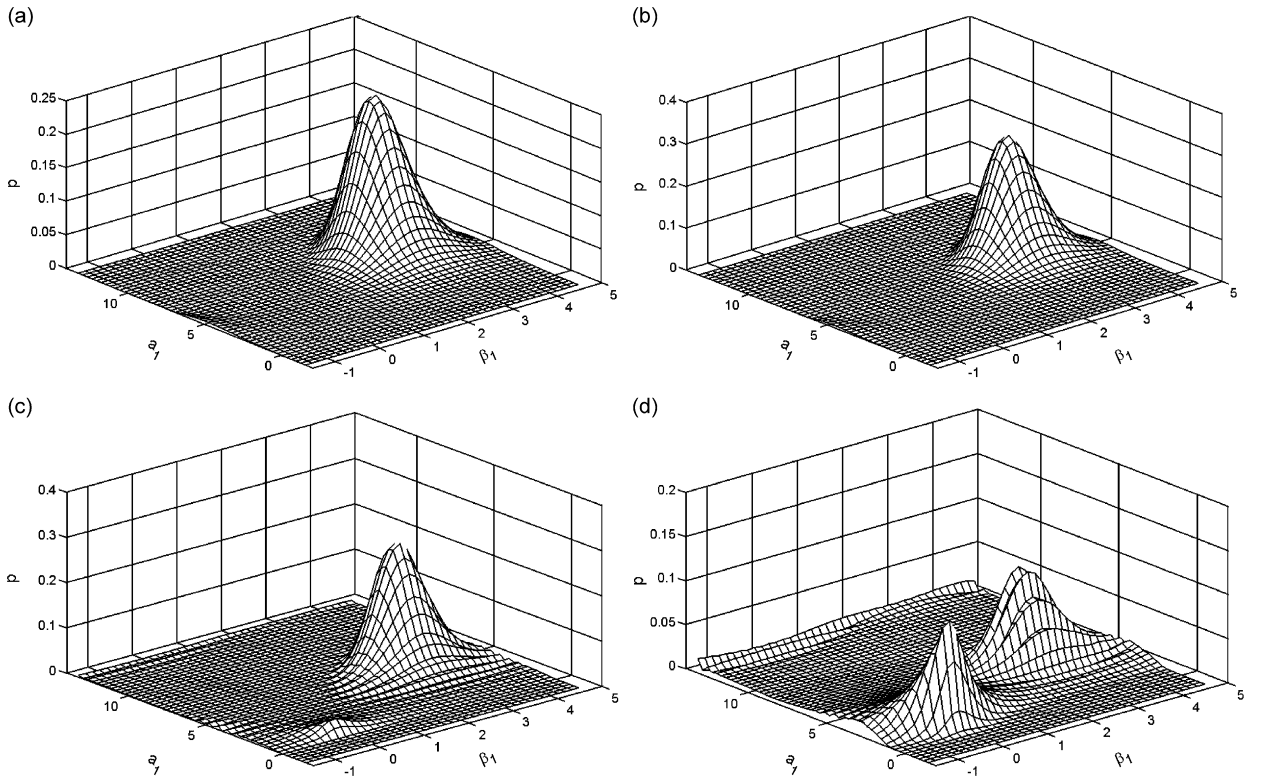

Fig. 14. Stationary joint probability density of the first mode to different excitation acceleration a: $\gamma = 0.01$; $f = 1.42$ Hz; (a) $a = 3.00\,\mathrm{m/s^2}$; (b) $a = 2.00\,\mathrm{m/s^2}$; (c) $a = 1.55\,\mathrm{m/s^2}$; and (d) $a = 1.40\,\mathrm{m/s^2}$.

the first-order moment frequency–response data (curves) or the first-order moment force–response data (curves) of the first two modes are all in agreement with the experimental results. From this point of view, the explanation on the importance of the nonlinear responses of a cantilever beam vertically excited by a modal shaker using narrow-band stochastic theory is reasonable and effective.

Furthermore, the stochastic jump and bifurcation have been investigated for the first modal parametric principal resonance by using the stationary joint probability of amplitude and phase to characterize the number, location, shape and magnitude of the peaks of the stationary joint probability density. Results show that stochastic jump occurs mainly in the region of triple-valued solution. For the frequency–response domain, if the bandwidth γ is a variable, the basic phenomena indicate that the most probable motion is around the higher branch when the bandwidth is smaller, whereas the most probable motion gradually approaches the lower one when the bandwidth becomes higher; if the excitation central frequency is a variable, the basic phenomena imply that the higher is the excitation central frequency f, the more probable is the jump from the higher branch to the lower one once f exceeds an certain value. For the force–response domain, there is a region of excitation acceleration a within which the joint probability density has two peaks: an upper peak and a lower peak. Results show that jumps may occur in this region where the response is also in the region of triple-valued solution. Concretely, as the value of a decreases, the upper peak decreases while the lower peak increases. Such phenomena indicate that the lower is the excitation acceleration a, the more probable is the jump from the higher branch to the lower one once a lies in the region.

Acknowledgment

This work was supported by National Natural Science Foundation of China under Grant no. 10572099.

References

[1] E.C. Haight, W.W. King, Stability of parametrically excited vibrations of an elastic rod, *Developments in Theoretical and Applied Mechanics* 5 (1971) 677–713.
[2] H.A. Evensen, R.M. Even-Iwanowski, Effects of longitudinal inertia upon the parametric response of elastic columns, *ASME Journal of Applied Mechanics* 33 (1966) 141–148.
[3] A.H. Nayfeh, D.T. Mook, *Nonlinear Oscillations*, Wiley, New York, 1979.

[4] M.R.M. Crespo Da Silva, C.C. Glynn, Non-linear flexural–flexural–torsional dynamics of inextensional beams—I: equations of motion, *Journal of Structural Mechanics* 6 (1978) 437–448.
[5] M.R.M. Crespo Da Silva, C.C. Glynn, Non-linear flexural–flexural–torsional dynamics of inextensional beams—II: forced motions, *Journal of Structural Mechanics* 6 (1978) 449–461.
[6] M.R.M. Crespo Da Silva, C.C. Glynn, Non-linear non-planar resonant oscillations in fixed-free beams with support asymmetry, *International Journal of Solids and Structures* 15 (1979) 209–221.
[7] M.R.M. Crespo Da Silva, Non-linear flexural–flexural–torsional–extensional dynamics of beams—I: formulation, *International Journal of Solids and Structures* 24 (1988) 1225–1234.
[8] M.R.M. Crespo Da Silva, Non-linear flexural–flexural–torsional–extensional dynamics of beams—II: response analysis, *International Journal of Solids and Structures* 24 (1988) 1235–1242.
[9] A.H. Nayfeh, P.F. Pai, Non-linear non-planar parametric responses of an inextensional beam, *International Journal of Non-Linear Mechanics* 24 (1989) 138–158.
[10] P.F. Pai, A.H. Nayfeh, Non-linear non-planar oscillations of a cantilever beam under lateral base excitations., *International Journal of Non-Linear Mechanics* 25 (1990) 455–474.
[11] H.N. Arafat, A.H. Nayfeh, C.M. Chin, Nonlinear nonplarnar dynamics of parametrically excited cantilever beams, *Nonlinear Dynamics* 15 (1998) 31–61.
[12] T.J. Anderson, A.H. Nayfeh, B. Balachandran, Experimental verification of the importance of the nonlinear curvature in the response of a cantilever beam, *ASME Journal of Vibration and Acoustics* 118 (1996) 21–27.
[13] L.D. Zavodney, A.H. Nayfeh, The non-linear response of a slender beam carrying a lumped mass to a principal parametric excitation: theory and experiment, *International Journal of Non-Linear Mechanics* 24 (1989) 105–125.
[14] R.C. Kar, S.K. Dwivedy, Non-linear dynamics of a slender beam carrying a lumped mass with principal parametric and internal resonances, *International Journal of Non-Linear Mechanics* 34 (1999) 515–529.
[15] S.K. Dwivedy, R.C. Kar, Dynamics of a slender beam with an attached mass under combination parametric and internal resonances—I: steady state response, *Journal of Sound and Vibration* 221 (1999) 823–848.
[16] S.K. Dwivedy, R.C. Kar, Dynamics of a slender beam with an attached mass under combination parametric and internal resonances—II: periodic and chaotic responses, *Journal of Sound and Vibration* 222 (1999) 281–305.
[17] S.K. Dwivedy, R.C. Kar, Non-linear dynamics of a slender beam carrying a lumped mass under principal parametric resonances with three-mode interaction, *International Journal of Non-Linear Mechanics* 36 (2001) 927–945.
[18] S.K. Dwivedy, R.C. Kar, Simultaneous combination principal parametric and internal resonances in a slender beam with a lumped mass: three-mode interactions, *Journal of Sound and Vibration* 242 (2001) 27–46.
[19] S.K. Dwivedy, R.C. Kar, Simultaneous combination and 1:3:5 internal resonances in a parametrically excited beam-mass system, *International Journal of Non-Linear Mechanics* 38 (2003) 585–596.
[20] T.R. Kane, R.R. Ryan, A.K. Banerjee, Dynamics of a cantilever beam attached to a moving base, *Journal of Guidance, Control, and Dynamics* 10 (1987) 139–151.
[21] H.H. Yoo, R.R. Ryan, R.A. Scott, Dynamics of flexible beams undergoing overall motions, *Journal of Sound and Vibration* 181 (1995) 261–278.
[22] S.H. Hyun, H.H. Yoo, Dynamic modeling and stability analysis of axially oscillating cantilever beams, *Journal of Sound and Vibration* 228 (1999) 543–558.
[23] S.S. Oueini, A.H. Nayfeh, Single-mode control of a cantilever beam under parametric excitation, *Journal of Sound and Vibration* 224 (1999) 33–47.
[24] K.A. Alhazza, M.F. Daqaq, A.H. Nayfeh, D.J. Inman, Nonlinear vibration of parametrically excited cantilever beams subjected to nonlinear delayed-feedback control, *International Journal of Non-Linear Mechanics* 43 (2008) 801–812.
[25] H. Rong, W. Xu, T. Fang, Principal response of Duffing oscillator to combined deterministic and narrow-band random parametric excitation, *Journal of Sound and Vibration* 210 (1998) 483–515.
[26] H.W. Rong, G. Meng, X.D. Wang, W. Xu, T. Fang, Largest Lyapunov exponent for second-order linear systems under combined harmonic and random parametric excitations, *Journal of Sound and Vibration* 283 (2005) 1250–1256.
[27] W.Q. Zhu, M.Q. Lu, Q.T. Wu, Stochastic jump and bifurcation of a Duffing oscillator under narrow-band excitation, *Journal of Sound and Vibration* 165 (1993) 285–304.
[28] H.W. Rong, W. Xu, X.D. Wang, G. Meng, T. Fang, Response statistics of two-degree-of-freedom non-linear system to narrow-band random excitation, *International Journal of Non-Linear Mechanics* 37 (2002) 1017–1028.
[29] H.G. Davies, G.V. Anand, Phase plane for narrow band random excitation of a Duffing oscillator, *Journal of Sound and Vibration* 104 (1986) 277–283.
[30] H.G. Davies, Q. Liu, The response envelope probability density function of a Duffing oscillator with random narrow band excitation, *Journal of Sound and Vibration* 139 (1990) 1–8.
[31] S. Rajan, H.G. Davies, Multiple time scaling of the response of a Duffing oscillator to narrow-band random excitation, *Journal of Sound and Vibration* 123 (1988) 497–506.
[32] H.G. Davies, S. Rajan, Random superharmonic and subharmonic response: multiple time scaling of a Duffing oscillator, *Journal of Sound and Vibration* 126 (1988) 195–208.
[33] Z.L. Huang, W.Q. Zhu, Y. Suzuki, Stochastic averaging of strongly non-linear oscillators under combined harmonic and white noise excitations, *Journal of Sound and Vibration* 238 (2000) 233–256.
[34] W.Q. Zhu, *Random Vibration*, Science Press, Beijing, 1992.
[35] Z.L. Huang, W.Q. Zhu, Stochastic averaging of quasi-integrable Hamiltonian systems under combined harmonic and white noise excitations, *International Journal of Non-Linear Mechanics* 39 (2004) 1421–1434.
[36] Z.L. Huang, W.Q. Zhu, Stochastic averaging of quasi-integrable Hamiltonian systems under bounded noise excitations, *Probabilistic Engineering Mechanics* 19 (2004) 219–228.
[37] Z.H. Feng, H.Y. Hu, Largest Lyapunov exponent and almost certain stability analysis of slender beams under a large linear motion of basement subject to narrow-band random parametric excitation, *Journal of Sound and Vibration* 257 (2002) 733–752.
[38] Z.H. Feng, X.J. Lan, X.D. Zhu, Principal parametric resonances of a slender cantilever beam subject to axial narrow-band random excitation of its base, *International Journal of Non-Linear Mechanics* 42 (2007) 1170–1185.
[39] R.L. Stratonovich, *Topics in the Theory of Random Noise*, Vol. II, Gordon and Breach, New York, 1967.
[40] M.F. Dimentberg, *Statistical Dynamics of Nonlinear and Time-Varying System*, Wiley, New York, 1988.
[41] W. Wedig, Analysis and simulation of nonlinear stochastic systems, in: W. Schiehlen (Ed.), *Nonlinear Dynamics in Engineering Systems*, Springer, Berlin, 1989, pp. 337–344.
[42] Y.K. Lin, G.Q. Cai, *Probabilistic Structural Dynamics: Advanced Theory and Applications*, McGraw-Hill, New York, 1995.
[43] S.T. Ariaratnam, Stochastic stability of viscoelastic systems under bounded noise excitation, in: A. Naess, S. Krenk (Eds.), *IUTAM Symposium on Advances in Nonlinear Stochastic Mechanics*, Kluwer Academic Publishers, Dordrecht, 1996, pp. 11–18.
[44] W.C. Xie, Moment Lyapunov exponents of a two-dimensional system under bounded noise parametric excitation, *Journal of Sound and Vibration* 263 (2003) 593–616.
[45] W.Q. Zhu, Z.L. Huang, J.M. Ko, Y.Q. Ni, Optimal feedback control of strongly non-linear systems excited by bounded noise, *Journal of Sound and Vibration* 274 (2004) 701–724.
[46] G.Q. Cai, C. Wu, Modeling of bounded stochastic processes, *Probabilistic Engineering Mechanics* 19 (2004) 197–203.

[47] H.W. Rong, X.D. Wang, W. Xu, T. Fang, Saturation and resonance of nonlinear system under bounded noise excitation, *Journal of Sound and Vibration* 291 (2006) 48–59.
[48] A.H. Nayfeh, S.J. Serhan, Response statistics of non-linear systems to combined deterministic and random excitations, *International Journal of Non-Linear Mechanics* 25 (1990) 493–509.
[49] M. Shinozuka, Simulation of multivariate and multidimensional random processes, *Journal of the Acoustical Society of America* 49 (1971) 357–367.
[50] M. Shinozuka, C.M. Jan, Digital simulation of random processes and its applications, *Journal of Sound and Vibration* 25 (1972) 111–128.